PRZEGLĄD SPAWALNICTWA
Welding
TECHNOLOGY REVIEW

DOI: https://doi.org/10.26628/simp.wtr.v96.1180.34-40

Original Article

The influence of abrasive finishing conditions on the surface texture of Inconel 939 elements made using the 3D printing LPBF method

Ewa Wojtiuk *[1], **Joanna Radziejewska** [1] **Michał Marczak** [1]

[1] Institute of Manufacturing Technology, Faculty of Mechanical and Industrial Engineering, Warsaw University of Technology, 85 Narbutta Street, 02-524 Warsaw, Poland, joanna.radziejewska@pw.edu.pl; michal.marczak@pw.edu.pl

*correspondence: ewa.wojtiuk.stud@pw.edu.pl

Received: 20.01.2024; Accepted: 19.03.2024; Published: 30.03.2024

Abstract: The article presents research on finishing treatment applied to components made of Inconel through 3D printing by Laser Powder Bed Fusion method. Vibration-abrasive machining was carried out using a supporting fluid and various shapes of abrasive. The effects of the processing conditions were analysed based on the surface roughness of the samples and mass loss. The obtained collective results were subjected to comparative analysis with the effects of vibratory-abrasive processing without the use of a processing fluid, as presented in the article. The research has shown that using vibration-abrasive processing, it is possible to reduce the height of surface irregularities by more than three times after four hours of treatment. The intensity of processing was the highest in the first hour of the process. The lowest roughness heights Ra = 1.8 μm were obtained using ceramic balls in the presence of a supporting fluid.

Keywords: vibration-abrasive processing; IN939; roughness; additive manufacturing; 3D printing post-processing

Introduction

Additive manufacturing (AM), also known as 3D printing, is a process of joining materials to make objects from 3D model data, usually layer upon layer, as opposed to subtractive manufacturing methodologies. This tool less manufacturing approach can give industry new design flexibility, reduce energy use, and shorten time to market [1]. 3D metal printing allows for the creation of complex shapes that would be difficult or impossible to achieve using traditional methods, [1] which leads to faster prototyping and design-to-production cycles. Through additive technology, it minimizes material waste as only the necessary material is used to create the object. 3D metal printing is economically beneficial for low-volume production or when individually tailored components are required. Manufacturing using 3D printing enables the production of durable yet lightweight structures, which is crucial in various industries such as aviation and automotive. The 3D printing materials refer to the substances used in the creation of 3D-printed objects. They come in a variety of forms, including filaments, resins, and powders, and can be made from a range of materials, including plastic, metal, and ceramic [2]. One of the popular AM metallic materials include Inconel, which is renowned for its high strength, excellent resistance to corrosion and oxidation, and high temperature resistance. One of the most commonly employed materials is Inconel 718 [3]. New promising alloy is Inconel 939 that has excellent oxidation resistance [4] due to the higher chromium content than the IN 738 alloy and high creep strength at elevated temperatures [5,6]. The aerospace and power industries use it extensively. LPBF (Laser Powder Bed Fusion) or PBF (Powder Bed Fusion) is one of the most popular metal 3D printing technologies. It is a type of DMLM (Direct Metal Laser Melting) technology. PBF is a group of AM technologies in which the energy source is selectively used to bind or melt powder particles, creating parts layer by layer [7]. The significant temperature differences and swift cooling inherent in this method of 3D printing technique can lead to certain flaws within the component's structure, described as: the formation of topologically close-packed (TCP) phases, directional grain growth, segregation of elements, high residual stresses, formation of porosities and lack of fusion (LOF) and micro-cracks [8,9]. Finishing processing after 3D printing is a crucial stage in the production process of printed objects, transforming raw 3D prints into finished products with the desired appearance, functionality, and quality. Regardless of the type of 3D printing technique used, it often involves the presence of layered structures and imperfections on the surfaces of objects and high surface roughness [10]. Finishing processing becomes an essential step in refining these prints, giving them aesthetic and functional properties. Various mechanical post-processing techniques can be applied to improve the surface, such as barrel finishing (BF), shot peening (SP), ultrasonic

shot peening (USP), and ultrasonic impact treatment (UIT) [11]. The most frequently used metal finishing methods are machining, grinding, and polishing. One of the simple and cheap abrasive finishing methods that allows for smoothing the surface is processing in container smoothing machines. Due to the high roughness and usually complex shapes of 3D printed elements, this type of processing has great potential as a finishing treatment, especially since various versions of it have been developed.

Adding vibratory-abrasive processing into the production process after 3D printing is crucial for achieving excellent finishing properties and geometric accuracy. This processing allows for the improvement of the finishing quality of metal components and the removal of potential surface defects that may occur during 3D printing. Vibration-abrasive machining is an advanced surface processing method that is playing an increasingly important role in the industry in the context of achieving good finish quality and processing precision. Research shows that vibro-abrasive machining is an effective method of rounding the edges and remove burrs formed after machining [12]. Despite the use of a soft material, vibratory-abrasive processing removed burrs from aluminium pipes used in the research.

In recent years, as technology and tools have developed, vibratory abrasive machining has become an important issue in the field of engineering and manufacturing. Vibratory-abrasive processing of metal components after 3D printing is an advanced method for the post-processing and finishing of items created through 3D printing. 3D printing enables the production of complex and precise metal structures such as AlSi10Mg where there are studies [11,13] reported significant strength and ductility variations of this material. Another material used in 3D printing is Hastelloy X where despite many advantages of the SLM method there are many lacks in quality of the surface [14]. Much of the improvement can be made to get the low surface roughness and high dimensional accuracy as well as high density by using high scanning speed in the SLM process [15], however these prints often require an additional processing step to achieve the desired parameters and surface quality.

In the context of container smoothing processes, the vibro-abrasive machining is one of the production techniques of the finished products with low surface roughness [16]. In vibratory-abrasive processing, special machining tools are used to smooth the surfaces of processed objects. The precise composition of the abrasive shapes is a trade secret of manufacturers, and only the type of binder is typically disclosed. There are various types of abrasive shapes, including: ceramic (porcelain and from so-called heavy zirconia porcelain); resin-bonded polyester; urea-based.

Different materials can be used in the post-processing. There are studies [17] shows the impact of the barrel finishing method on the materials such as Ti6Al4V and Inconel 718, where it has a notable impact on the surface roughness. When these materials undergo barrel finishing, there is a remarkable improvement in their surface quality. It was important to know first the suitable process parameters to get the better quality of the surface [17,18].

Vibratory-abrasive processing can be applied together with an assistive fluid to enhance the surface quality of the processed material. Processing fluids are concentrates of various chemical compounds dissolved in water, which may also be present in the form of mixtures of solid chemical compounds. Assistive fluids must ensure good miscibility and solubility in water, as well as effective wetting of the processed surfaces, shapes, and walls of the working container. Chemically active components found in assistive fluids are most commonly inorganic and organic acids, including fatty acids, contributing to an acidic reaction (pH=1-3). Chemically active assistive fluids can also have an alkaline reaction (pH=9-11). Chemically active products are also the result of reactions between individual components in machining fluids, such as esters [19].

The aim of the research is to assess the impact of the vibro-abrasive processing conditions of 3D printed elements made of the difficult-to-machine Inconel 939 material on the surface roughness. The research analysed the influence of the type of abrasive shapes, machining time and the presence of machining fluid on the process efficiency and surface texture.

Materials and Methods

Using the Laser Powder Bed Fusion method, samples pictured in Fig. 1. were made. The production utilized a 3D printer, EOS M 100. The material from which all samples are made is Inconel 939, whose composition is presented in Tab. I Inconel 939 is a nickel-chromium alloy that provides a balance between high-temperature strength, corrosion resistance, and oxidation resistance. After printing the elements, heat treatment was carried out. According to the manufacturer's recommendations [20], saturation at a temperature of 1340 °C for 4 h followed by aging at 1000 °C for 6 h and 800 °C for 4 h were used.

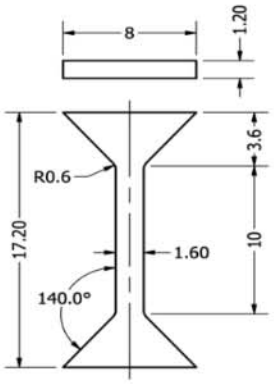

Fig. 1. Shape and dimensions of sample made of Inconel 939

The Inconel 939 samples underwent vibratory-abrasive treatment with the additional use of the processing fluid ROLLKEMIK FE-L 120-B32. The product used is dedicated to finishing and polishing of ferrous materials and additionally contains antioxidants. The pH value is 8.4. It is recommended for use with ceramic, porcelain, and shot shape fittings.

Each sample was assigned a specific type of fittings, as shown in Tab. I. The process consisted of four stages lasting one hour each. The processing station consists of six chambers, to which the media were assigned in order. Identical process parameters were used for all processing variants, the vibration amplitude was 1.4 mm.

Table I Description of the fittings used along with the assigned descriptions of the samples

Type of media	Appearance	Size	Mass [g]
Ceramic rollers		ø4.1 x 14.5	0.5
Porcelain rollers EB 0410 VZ		ø9.5	0.37
Ceramic rollers CB 0410 VH		ø4.1 x 11.5	0.31
Resin cones		ø11 x 11	0.75
Ceramic balls		ø6	1

After each treatment, the samples were cleaned in an ultrasonic cleaner for 3 minutes. Subsequently, the mass loss was checked using a WPS 50/C/2 scale (Radwag, Poland) and observations were made using a Keyence confocal laser microscope. The final step was a triple measurement of the roughness of each sample on a Taylor Hobson profilometer, from which the average roughness value Ra was calculated.

Results

Roughness tests after 3D printing showed that the surface is characterized by high irregularities. The Ra parameter ranged from 4.06 to 6.03 um and was characterized by large scatters (Tab. II). Figure 2a shows a photo of the post-printing surface. There is a layer of oxides and spherical particles with a size of several dozen micrometres attached to the substrate. Height of the irregularities determine surface roughness (Fig. 2b).

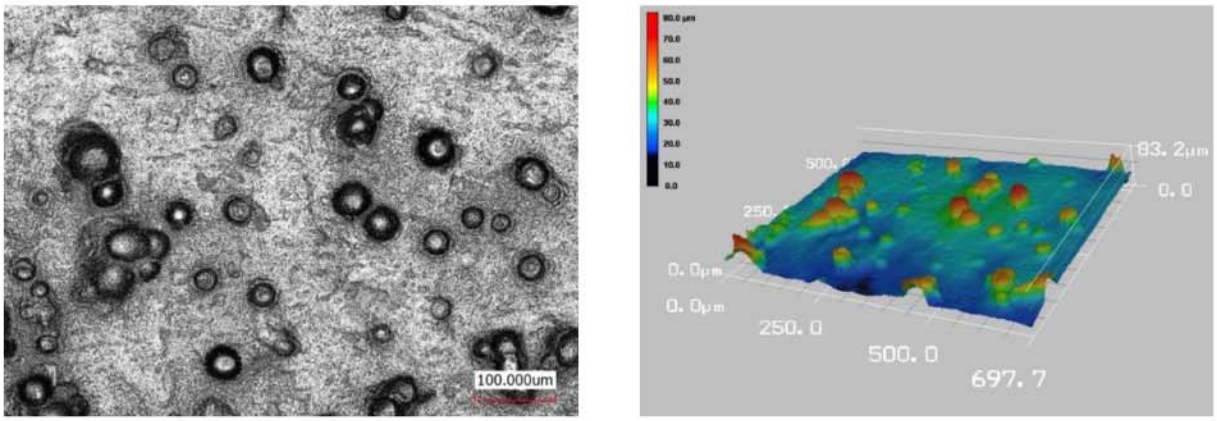

(a) (b)

Fig. 2. Surface of Inconel 939 after LPBF a) - photo b) -3D view; confocal microscope

After each hour of vibratory-abrasive treatment, the mass loss of each sample was measured and shown in Tab. II. Analyzing the mass loss for given samples, the largest mass loss occurred for the samples with cubes and ceramic balls media, and the smallest mass loss for the sample with resin cones media. For each of the samples, a significant mass loss is observed from hour to hour. The cube fittings have the biggest mass, each cube weighs 3.8 g and this type of media results in the largest mass loss for samples. The second type of fittings that results in large mass loss are ceramic balls, where one ceramic ball weighs 1 g.

Table II Change in mass for individual samples in each time interval for different type of shapes

Type of shapes	Initial mass [g]	Mass after 1h [g]	Mass after 2h [g]	Mass after 3h [g]	Mass after 4h [g]
Ceramic rollers	0.5181	0.5167	0.5153	0.5134	0.5127
Porcelain rollers EB 0410 VZ	0.5178	0.5154	0.5146	0.5139	0.5129
Ceramic rollers CB 0410 VH	0.5182	0.5155	0.5155	0.514	0.5135
Resin cones	0.5161	0.5147	0.5136	0.5118	0.5116
Ceramic balls	0.5109	0.5073	0.5062	0.5044	0.5032
Cubes	0.5206	0.517	0.5158	0.5139	0.5129

Each sample was measured on a profilometer in three different places, and then the data collected in this way was averaged and presented as well as total mass loss of samples for individual types of fittings. For comparison, the values from machining without the use of supporting fluid are included.

Table III Values of the roughness parameter Ra for vibration-abrasive machining without the use of machining fluid

Type of fittings	Ra-initial	Ra after 1h	Ra after 2h	Ra after 3h	Ra after 4h
Ceramic rollers	5.67	2.88	1.83	1.65	1.64
Porcelain rollers EB 0410 VZ	5.67	3.74	1.79	1.72	1.87
Ceramic rollers CB 0410 VH	5.67	3.02	2.48	2.22	1.92
Resin cones	6.03	5.63	3.65	3.81	3.18
Ceramic balls	4.06	1.66	1.54	1.3	1.4

Table II Values of the roughness parameter Ra for vibration-abrasive machining using a machining fluid

Type of fittings	Ra initial	Ra after 1h	Ra after 2h	Ra after 3h	Ra after 4h
Ceramic rollers	6.62	4.83	2.64	2.21	2.01
Porcelain rollers EB 0410 VZ	6.62	3.54	3.03	2.66	2.59
Ceramic rollers CB 0410 VH	6.62	3.68	2.84	2.84	2.48
Resin cones	6.62	2.84	2.80	2.16	2.23
Ceramic balls	6.62	2.08	1.73	1.95	1.81

Table V Comparative summary of the difference between the initial and final value of the Ra parameter for treatment with and without fluid

Type of fittings	Δ Ra for treatment without fluid	Δ Ra for treatment with fluid
Ceramic rollers	4.03	4.60
Porcelain rollers EB 0410 VZ	3.8	4.02
Ceramic rollers CB 0410 VH	3.75	4.13
Resin cones	2.85	4.38
Ceramic balls	2.66	4.81

Analyzing the obtained roughness parameters Ra from Tab. III and Tab. IV, it is noticeable that the Ra final values (after 4 hours of processing) are significantly lower for the elements processed without the use of processing fluid compared to those processed with this fluid, except for the samples subjected to the process with resin cones fittings. However, considering the roughness values of the tested elements before the process and after the entire treatment, a significantly greater difference occurs in the case of elements processed with the use of supporting fluid, as illustrated in Tab. V. Regardless of the type of media, a significant improvement in the Ra value occurred in the case of vibratory-abrasive processing using processing fluid.

Fig. 3 shows a photo and view of the surface after four hours of vibro-abrasive treatment using ceramic rollers. The complete removal of particles from the surface and the smoothing of the irregularities as a result of the friction of the shapes against the surface of the samples are visible.

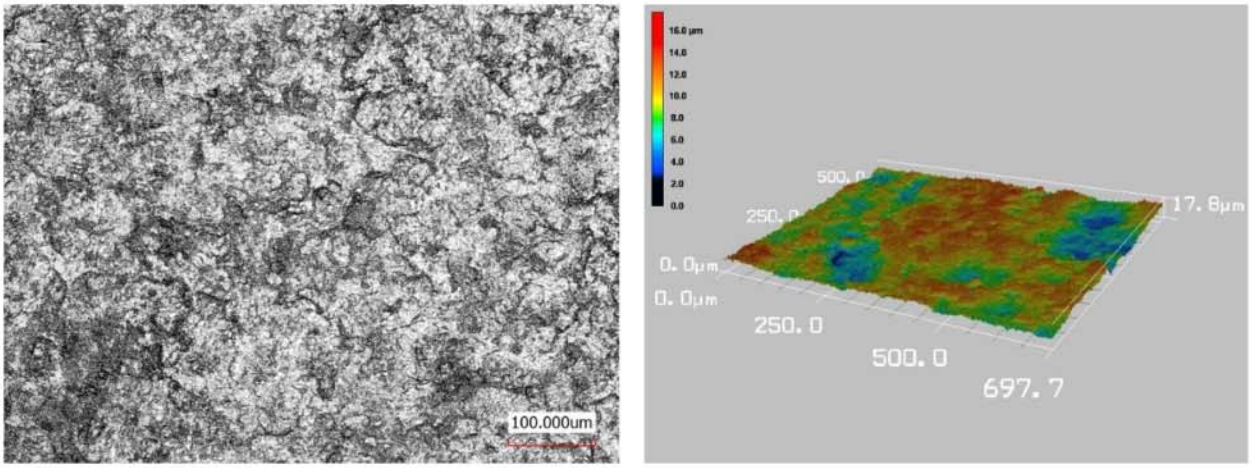

(a) (b)

Fig. 3. Surface of Inconel 939 after LPBF a and vibro-abrasive treatment using a) - photo b) -3D view; confocal microscope

Table VI Total mass loss of samples for individual types of fittings after machining with and without the assistance of a machining fluid

Type of fittings	Mass loss [g] of samples with fluid assistance	Mass loss [g] of samples without fluid assistance
Ceramic rollers	0.0054	0.0070
Ceramic rollers EB 0410 VZ	0.0049	0.0082
Ceramic rollers CB 0410 VH	0.0047	0.0096
Resin cones	0.0045	0.0038
Ceramic balls	0.0077	0.0065

Compare the mass loss of the tested elements subjected to the vibratory-abrasive processing with and without liquid assistance. Analyzing the Tab. VI it is evident that the process conducted without the use of processing fluid, utilizing ceramic and porcelain cylinder media, leads to a greater mass loss of samples compared to the process performed with supporting liquid. In the case of ceramic rollers CB 0410 VH media

for processing without the use of processing fluid, the samples lost twice as much mass (precisely 2.049 times) than those samples processed with the same media along with supporting liquid.

In the case of resin cones and ceramic balls shapes, the processed samples lost more mass in the process with the support of processing liquid than without. The difference was 0.00067 g for processing with resin cones and 0.001163 g for ceramic balls.

Summary

The research has shown that because of using vibro-abrasive processing, it is possible to reduce the height of surface irregularities after 3D printing by more than three times after four hours of treatment. Material loss and roughness reduction are the most intense in the first hour of the process for all tested variants of fittings, regardless of the use of cutting fluid. During this period, the surface is smoothed mainly by detaching less strongly bonded particles on the surface of the samples. In the following hours of the process, the mass loss results mainly from the process of friction of the shapes on the sample surface. The conducted research indicates that the type of fittings used has a greater impact on the process than the presence of the supporting fluid. The lowest roughness was obtained when using ceramic balls, for machining without fluid Ra was 1.4 μm and in the presence of fluid it was 1.8 μm. The presence of fluid reduces the friction coefficient and material loss is less intense.

From the data obtained, it emerged that elements processed with processing fluid using ceramic balls shaped fittings, for the Inconel 939 samples, show the greatest improvement in the geometric structure of the surface and experience the greatest mass loss.

Comparing the results of the surface roughness values of the tested samples obtained from container processing with and without the use of a supporting fluid, it appears that a specific type of fittings should be used for a specific type of processing. In the case of using ceramic or porcelain shapes of fittings, abrasive processing without supporting fluid is significantly better. However, considering resin cones and ceramic balls shape, slightly better results were obtained during processing with supporting fluid than without it. An important aspect are also the obtained roughness values of the tested samples, where it is not possible to unequivocally determine which of the processing methods is the best, whether with the use of supporting fluid or without. As a comparison to the research [18] it was shown that using ceramic pellet shapes and machining fluid significantly reduces the average surface roughness Ra, from 6 μm to 1.2 μm. Another important aspect determining the improvement of the sample surface is not only the shape of the fittings but also the weight of the individual one of them. As in the research [18] it was claimed that the weight of the abrasive shapes, exerts the most significant influence on the surface roughness of the vibratory finishing process.

Depending on which of the methods is chosen, it is necessary to select the appropriate type of fittings for it to achieve the best possible result. Further research is necessary on both methods of vibratory-abrasive machining - with and without fluid - using various shapes to determine the impact of machining conditions on the surface layer integrity and the mechanical properties of the elements.

Author Contributions: Conceptualization, E.W. and J.R.; methodology, E.W. and J.R.; software, E.W.; validation, E.W., J.R. and M.M.; formal analysis, J.R.; investigation, E.W. and M.M.; resources, J.R.; data curation, E.W.; writing—original draft preparation, E.W. and J.R.; writing—review and editing, E.W.; visualization, E.W. and M.M.; supervision, J.R.; project administration, J.R.; funding acquisition, J.R.
Conflicts of Interest: The authors declare no conflict of interest.

References

1. Shaikh, A.S.; Rashidi, M.; Minet-Lallemand, K.; Hryha, E. On as-built microstructure and necessity of solution treatment in additively manufactured Inconel 939. *Powder Metall.* **2023**, *66*, 3–11, doi:10.1080/00325899.2022.2041787.
2. Diniță, A.; Neacșa, A.; Portoacă, A.I.; Tănase, M.; Ilinca, C.N.; Ramadan, I.N. Additive Manufacturing Post-Processing Treatments, a Review with Emphasis on Mechanical Characteristics. *Materials (Basel).* **2023**, *16*, 4610, doi:10.3390/ma16134610.
3. Hosseini, E.; Popovich, V.A. A review of mechanical properties of additively manufactured Inconel 718. *Addit. Manuf.* **2019**, *30*, 100877, doi:10.1016/j.addma.2019.100877.
4. González, M.A.; Martínez, D.I.; Pérez, A.; Guajardo, H.; Garza, A. Microstructural response to heat affected zone cracking of prewelding heat-treated Inconel 939 superalloy. *Mater. Charact.* **2011**, *62*, 1116–1123, doi:10.1016/j.matchar.2011.09.006.
5. Kanagarajah, P.; Brenne, F.; Niendorf, T.; Maier, H.J. Inconel 939 processed by selective laser melting: Effect of

microstructure and temperature on the mechanical properties under static and cyclic loading. *Mater. Sci. Eng. A* **2013**, *588*, 188–195, doi:10.1016/j.msea.2013.09.025.

6. Shaikh, A.S. Development of a γ′ Precipitation Hardening Ni-Base Superalloy for Additive Manufacturing, Chalmers University of Technology, 2018.
7. Li, X.; Shi, J.J.; Wang, C.H.; Cao, G.H.; Russell, A.M.; Zhou, Z.J.; Li, C.P.; Chen, G.F. Effect of heat treatment on microstructure evolution of Inconel 718 alloy fabricated by selective laser melting. *J. Alloys Compd.* **2018**, *764*, 639–649, doi:10.1016/j.jallcom.2018.06.112.
8. Liu, P.; Hu, J.; Sun, S.; Feng, K.; Zhang, Y.; Cao, M. Microstructural evolution and phase transformation of Inconel 718 alloys fabricated by selective laser melting under different heat treatment. *J. Manuf. Process.* **2019**, *39*, 226–232, doi:10.1016/j.jmapro.2019.02.029.
9. Lesyk, D.A.; Martinez, S.; Mordyuk, B.N.; Dzhemelinskyi, V. V.; Lamikiz; Prokopenko, G.I. Post-processing of the Inconel 718 alloy parts fabricated by selective laser melting: Effects of mechanical surface treatments on surface topography, porosity, hardness and residual stress. *Surf. Coatings Technol.* **2020**, *381*, 125136, doi:10.1016/j.surfcoat.2019.125136.
10. Duda, T.; L. Venkat, R. 3D Metal Printing Technology. In Proceedings of the IFAC Papers Online Conference Paper Archive, 49-29; 2016; pp. 103–110.
11. Serjouei, A.; Libura, T.; Brodecki, A.; Radziejewska, J.; Broniszewska, P.; Pawłowski, P.; Szymczak, T.; Bodaghi, M.; Kowalewski, Z.L. Strength-hardness relationship for AlSi10Mg alloy produced by laser powder bed fusion: An experimental study. *Mater. Sci. Eng. A* **2022**, doi:10.1016/j.msea.2022.144345.
12. Bańkowski, D.; Spadło, S. The influence of abrasive paste on the effects of vibratory machining of brass. *Arch. Foundry Eng.* **2019**, *19*, 5–10, doi:10.24425/afe.2019.129622.
13. Kamarudin, K.; Wahab, M.S.; Shayfull, Z.; Ahmed, A.; Raus, A.A. Dimensional Accuracy and Surface Roughness Analysis for AlSi10Mg Produced by Selective Laser Melting (SLM). In Proceedings of the MATEC Web of Conferences; 2016; p. 01077.
14. Tian, Y.; Tomus, D.; Rometsch, P.; Wu, X. Influences of processing parameters on surface roughness of Hastelloy X produced by selective laser melting. *Addit. Manuf.* **2017**, *13*, 103–112, doi:10.1016/j.addma.2016.10.010.
15. Han, X.; Zhu, H.; Nie, X.; Wang, G.; Zeng, X. Investigation on selective laser melting AlSi10Mg cellular lattice strut: Molten pool morphology, surface roughness and dimensional accuracy. *Materials (Basel).* **2018**, *11*, 392, doi:10.3390/ma11030392.
16. Damian, B.; Daniel, K.; Piotr, M. Deburring and Smoothing the Edges Using Vibro-abrasive Machining. *Procedia Eng.* **2017**, *192*, 28–33, doi:10.1016/j.proeng.2017.06.005.
17. Boschetto, A.; Bottini, L.; Macera, L.; Veniali, F. Post-processing of complex SLM parts by barrel finishing. *Appl. Sci.* **2020**, *10*, 1382, doi:10.3390/app10041382.
18. Radziejewska, J.; Marczak, M.; Maj, P.; Głowacki, D. The Influence of Vibro-Assisted Abrasive Processing on the Surface Roughness and Sub-Surface Microstructure of Inconel 939 Specimen Made by LPBF. *Materials (Basel).* **2023**, *16*, 7429, doi:10.3390/ma16237429.
19. Woźniak, K. *Obróbka powierzchni w wygładzarkach pojemnikowych*; 2017; ISBN 978-83-01-19205-1.
20. Metal Solutions: EOS Nickel Alloy IN939 Material Data Sheet Metal Solutions Available online: https://www.eos.info/05-datasheet-images/Assets_MDS_Metal/EOS_NickelAlloy_IN939/Material_DataSheet_EOS_NickelAlloy_IN939_en.pdf.